RESEARCH ARTICLE
doi: 10.2306/scienceasia1513-1874.2025.028

ScienceAsia 51 (2): 2025: ID 2025028: **1–10**

Caspase-1 inhibitor VX-765 alleviates $PM_{2.5}$-induced hepatic lipid metabolism disorder in mice

Sisi Qin[a], Lei Wu[b], Yongheng Wang[a,c], Ning Li[a], Changyu Qin[a], Shoufang Jiang[a], Jianfen Wei[d], Naijun Wu[d], Fuyuan Cao[a,e,*], Shuang Li[a,c,e,*]

[a] School of Public Health, North China University of Science and Technology, Hebei 063210 China
[b] School of Psychology and Mental health, North China University of Science and Technology, Hebei 063210 China
[c] Hebei Key Laboratory of Organ Fibrosis Research, North China University of Science and Technology, Hebei 063210 China
[d] Department of Endocrinology, North China University of Science and Technology Affiliated Hospital, Hebei 063210 China
[e] Animal Experimental Center, North China University of Science and Technology, Hebei 063210 China

*Corresponding authors, e-mail: c-fuyuan@163.com, lishuangdwzx@ncst.edu.cn

Received 18 Jul 2024, Accepted 7 Feb 2025
Available online 22 Apr 2025

ABSTRACT: Long-term exposure to $PM_{2.5}$ is associated with hepatic lipid metabolism disorders, in which caspase-1 is involved, but the mechanism is not fully understood. This study focused on the role of the caspase-1 inhibitor VX-765. A long-term $PM_{2.5}$ exposure model was constructed by concentrating ambient air particles. Mice were intraperitoneally administered with VX-765. The body weight, liver index, blood lipid, and hepatic disorder indices were measured. Hematoxylin and eosin staining, immunohistochemical staining, Western blot analysis, and real-time quantitative polymerase chain reaction were employed to assess histopathological changes and quantify the expression levels of target proteins and mRNAs. The results indicated that VX-765 could inhibit hepatic disorder, improve body weight and liver index, and regulate lipid metabolism by affecting the expression of key factors such as *caspase-1*, *IL-1β*, *SREBP-1*, *PPAR-α*, *PPAR-γ*, and *PDK4*. In conclusion, caspase-1 inhibitors offer a novel approach for alleviating hepatic disorder caused by long-term $PM_{2.5}$ exposure.

KEYWORDS: caspase-1, $PM_{2.5}$, caspase inhibitor, hepatic disorder, lipid metabolism

INTRODUCTION

Particulate matter 2.5 ($PM_{2.5}$), with a size smaller than 2.5 μm, constitutes a major portion of atmospheric particulate matter. It ranks as the fifth leading cause of global mortality and significantly contributes to the global disease burden [1]. In Hebei Province, China, coal consumption is high due to energy-intensive industries like steel production, petrochemicals, and building materials [2]. This makes Hebei a primary source of $PM_{2.5}$. Epidemiological and clinical studies have shown that $PM_{2.5}$ exposure first affects the lungs and then spreads to other organs via the bloodstream with the liver being an important target organ as it plays a vital role in metabolizing drugs and toxins [3, 4].

Lipids are essential nutrients for maintaining energy homeostasis and are constituents of cells and tissues [5]. Previous research has demonstrated that ambient $PM_{2.5}$ exposure can disrupt hepatic lipid metabolism with the dysregulation of enzymes involved in lipid metabolism (such as those related to lipogenesis, lipolysis, and fatty acid oxidation) being the molecular basis for this disruption [6]. Moreover, $PM_{2.5}$ has been found to induce pyroptosis through the activation of the classic NOD-like receptor pyrin domain containing 3 (NLRP3)-Cysteinyl aspartate specific proteinase-1 (caspase-1)-Gasdermin D protein (GSDMD) pathway, which involves the activation of caspase-1 and an increased release of Interleukin-1β (IL-1β). This provides evidence for targeting the caspase-1/IL-1β pathway, which is crucial in $PM_{2.5}$-induced pyroptosis and inflammatory responses [7]. Currently, there is limited research on hepatic metabolism induced by $PM_{2.5}$, highlighting the need for further study.

Caspase-1, a cysteine-containing enzyme, plays an essential role in the inflammasome and is involved in generating active IL-1β and Interleukin-18 (IL-18) by breaking down their initial forms. It also has a role in regulating body weight and glucose homeostasis [8]. Caspase-1 has wide substrate specificity beyond inflammation in metabolic pathways, suggesting it may have different roles in the body. It targets different metabolic pathways, including lipid metabolism, where it can modulate genes involved in lipid metabolism or regulate it through cytokine action [9]. VX-765 is an acknowledged inhibitor of caspase-1, which is a prodrug of VRT-043198 and can be taken orally. By acting on peripheral blood mononuclear cells, it hinders the secretion of IL-1β and IL-18 when stimulated by lipopolysaccharide (LPS) [10].

Given the established link between $PM_{2.5}$ exposure and hepatic disorder, this study aims to elucidate the molecular mechanisms underlying $PM_{2.5}$-induced liver

lipid metabolic disorder and investigate whether VX-765 could mitigate hepatic damage caused by $PM_{2.5}$ through the regulation of lipid metabolism.

MATERIALS AND METHODS

Animal source and grouping

Forty male C57BL/6 SPF grade mice, weighing 18–20 g, were accommodated in barrier environmental facilities at the Animal Experimental Center of the North China University of Science and Technology [LAEC-NCST-2020109; China], maintaining a temperature range of 21 to 24 °C, relative humidity of 50%, and a consistent 12 h cycle of day and night. All mice had access to standard chow and distilled water. Four groups of mice (Control: Filtered Air Exposure group, PM: Concentrated $PM_{2.5}$ Air Exposure group, PV: Concentrated $PM_{2.5}$ Air Exposure+VX-765 Intervention group, and VX: Filtered air exposure + VX-765 intervention group) were randomly selected after a seven-day acclimatization period. The weight of the mice was recorded on a weekly basis. Details of the reagents and instruments used in this study are provided in Table S1 and Table S2 of the Supplementary Materials.

Animal exposure and intervention

The mice in the PM and PV groups were subjected to the dynamic inhalation exposure chambers of the exposure system, where the concentration of $PM_{2.5}$ was 8 times higher than the outdoor concentration, 6 h per day, 7 days per week. The mice in the Control and VX groups were accommodated in a dedicated ventilated cage feeding system with a $PM_{2.5}$ concentration of 0 units. The exposure period spanned from October 15, 2022, to January 1, 2023, totaling 100 days. The VX-765, a caspase-1 inhibitor, was administered to the mice in the PV and VX groups at a dose of 50 mg/kg. The administration was carried out by intraperitoneal injection once every 3 days, commencing from the onset of the exposure and persisting throughout the entire 100-day period. In the clean air exposure group (Con) and $PM_{2.5}$ concentrated air exposure (PM), mice received an intraperitoneal injection of an equal 0.9% volume of saline with the same intervention method and frequency as the PV and VX groups. At the conclusion of the exposure experiments, the mice were anesthetized with 1% sodium pentobarbital. Subsequently, the liver was rinsed with a solution of saline and phosphate buffers. Sections of the liver were either preserved for histological evaluation or rapidly frozen for additional biochemical testing.

Biochemical indicator

The levels of serum total cholesterol (TC), triglyceride (TG), aspartate aminotransferase (AST), alanine aminotransferase (ALT), high-density lipoprotein (HDL), and low-density lipoprotein (LDL) were measured using an automated biochemical analyzer.

Histopathological examination and immunohistochemical staining

In order to perform a histological examination, the liver tissue was extracted and stored in 4% paraformaldehyde for at least 24 h. Afterward, the preserved tissues were embedded in paraffin, sliced at a thickness of 4 µm, and mounted on glass slides. The liver tissue was then stained with Hematoxylin and eosin (HE). Also, the liver tissue samples were subjected to immunohistochemical (IHC) staining to detect the presence of specific protein levels of caspase-1, Peroxisome Proliferator-Activated Receptor-α (PPAR-α), Peroxisome Proliferator-Activated Receptor-γ (PPAR-γ), and Pyruvate Dehydrogenase Kinase 4 (PDK4).

Western blot (WB) analysis

Total proteins extracted from liver tissues were quantified and denatured in a loading buffer at high temperatures. To prevent repeated freezing and thawing cycles, frozen protein samples were stored separately at −20 °C. For electrophoresis, we used an SDS-PAGE system containing sodium dodecyl sulfate to separate the proteins based on their size. The proteins were then transferred to prewetted nitrocellulose membranes using a buffer optimized for membrane transfer. To minimize nonspecific antibody binding, the membranes were blocked with Tris-buffered saline containing 5% skim milk overnight. Following blocking, primary antibodies that target caspase-1, IL-1β, cluster of differentiation 36 (CD36), and SREBP-1 were used to incubate the membranes to detect their expression levels. After incubating with the primary antibody, the membranes were washed with Tris-Buffered Saline (TBS) to remove unbound antibodies. Secondary antibodies conjugated with a fluorescent marker were then applied for 1 h to enable the visualization of the protein bands. The protein bands were identified and measured utilizing the Li-Cor Odyssey imaging system. ImageJ software (NIH, Bethesda, MD, USA) was utilized for the quantitative analysis of fluorescence density, allowing for precise measurement of the expression levels of the target proteins.

Quantitative real-time polymerase chain (qPCR) reaction

The RNA extraction kit was employed for the isolation of total RNA from the liver tissues in accordance with the instructions outlined by the manufacturer. The reverse transcription process was conducted using the PrimeScript RT Master Mix. The mRNA levels of *caspase-1*, *CD36*, *PPAR-α*, *PPAR-γ*, *SREBP-1*, *PDK4*, and *β-actin* were measured using a real-time quantitative

fluorescent RNA amplification machine. The amplification procedure was performed as follows: initial denaturation at 95 °C for 3 min; followed by 40 cycles of denaturation at 95 °C for 15 s, annealing/extension at 60 °C for 1 min. The relative expression of target genes was calculated using the $2^{-\Delta\Delta Ct}$ method. The primers (see Table S3 presented in the Supplementary Materials) were designed by Sangon Biotech Company (Shanghai, China). Then, Sanger sequencing was performed on qPCR products generated with divergent primers.

Statistical analysis

Data analysis was performed using SPSS 23.0. For small-sample multi-group measurement data, the Shapiro-Wilk normality test was conducted first. If all data were normally distributed, they were represented by mean±standard deviation. Otherwise, the interquartile range was used. For comparison of 2 groups of data, a normality test was performed first. If the data were normally distributed, an independent sample *t*-test was used. Before the *t*-test, a homogeneity of variance test (Levene Statistic) was conducted. If the variances were homogeneous, the *t*-test was directly performed. If the variances were not homogeneous, a correction method (such as Welch's *t*-test) was used. For multi-group normal measurement data, one-way ANOVA was used. First, a homogeneity of variance test was conducted. If the variances were homogeneous, *F*-test and SNK pairwise comparisons were used. If the variances were not homogeneous, Welch's *t*-test and Dunnett's *T3* pairwise comparisons were used (if there was no significance, no pairwise comparison was made). For multi-group non-normal measurement data, Kruskal-Wallis one-way ANOVA was used for pairwise comparisons. GraphPad Prism 9 software was used for plotting. A p-value less than 0.05 was considered statistically significant.

RESULTS

Exposure concentration of particulate matter ($PM_{2.5}$)

From September 25, 2022, to March 1, 2023, the average concentration of $PM_{2.5}$ in the Animal Experimental Center of North China University of Science and Technology was about 43.34 μg/m^3. During 100 days of $PM_{2.5}$ exposure, the average concentrations in the Con and PM rooms were 0 and 346.9 μg/m^3, respectively. Particulate matter smaller than 0.25 micrometers was not detected in the Con chamber in our study either. The detection rates of particulate matter below 2.5 μm were 99.59% in the PM chambers.

Long-term exposure to $PM_{2.5}$ induces hepatic disorder

As shown in Fig. 2(a–h), after 100 days of $PM_{2.5}$ exposure, a remarkable decrease in weight and a significant increase in liver coefficients were observed ($p < 0.05$). The above results indicated that the metabolism of mice was affected by $PM_{2.5}$, resulting in weight loss and increased liver weight. Meanwhile, the levels of TC, TG, AST, ALT, and LDL in serum were significantly higher, while that of HDL in serum was significantly lower in the PM group than in the Con group. The changes in biochemical markers indicated that the accumulation of excess triglycerides, increased adipose tissue, and metabolic disorders were caused by long-term exposure to $PM_{2.5}$. As shown in Fig. 2(i), histopathological observation of liver tissues revealed that a large number of lipid droplets appeared, cloudy swelling of hepatocytes significantly increased, and inflammatory cell infiltration occurred in hepatocytes after exposure to $PM_{2.5}$. Therefore, a conclusion consistent with other research findings can be drawn that the induction of $PM_{2.5}$ makes the liver more prone to lipid accumulation.

Long-term exposure to $PM_{2.5}$ activates lipid metabolic pathways to promote hepatic disorder

To elucidate the effect of $PM_{2.5}$ exposure on lipid metabolism at the molecular level, the expression of key genes and their corresponding proteins involved in lipid metabolic processes, namely caspase-1, IL-1β, PDK4, CD36, SREBP-1, PPAR-α, and PPAR-γ, were focused on, as shown in Fig. 3. In the context of WB, which detects protein levels, the relative amounts of the target proteins are reflected by the band intensities. In the WB results, compared with the control group, the PM group showed a significant upregulation of caspase-1 protein, IL-1β protein, CD36 protein, and SREBP-1 protein ($p < 0.05$). These WB results validated the changes in protein expression levels induced by $PM_{2.5}$ exposure. Regarding qPCR analysis, which measures mRNA levels of genes, the qPCR results exhibited a similar trend to the protein expression levels detected by WB. Specifically, the mRNA expressions of *PPAR*-α and *PPAR*-γ in the PM group decreased ($p < 0.05$), while a significant upregulation of *PDK4* mRNA was evident ($p < 0.05$), indicating that lipid metabolism at the transcriptional level is also affected by $PM_{2.5}$ exposure. Regarding IHC, significant importance is held by the brownish indication. In the context of IHC, the presence and distribution of the target proteins under investigation are indicated by the brownish color. A higher expression level of these proteins may be suggested by a stronger brownish staining intensity. In the PM group exposed to $PM_{2.5}$, the alterations in protein expression levels caused by $PM_{2.5}$ are understood with the help of the changes in the brownish indication. In this experiment, consistency between the trend of IHC and that of WB and PCR is observed. Additionally, crucial evidence for understanding the molecular mechanisms underlying $PM_{2.5}$-induced changes in lipid metabolism is provided

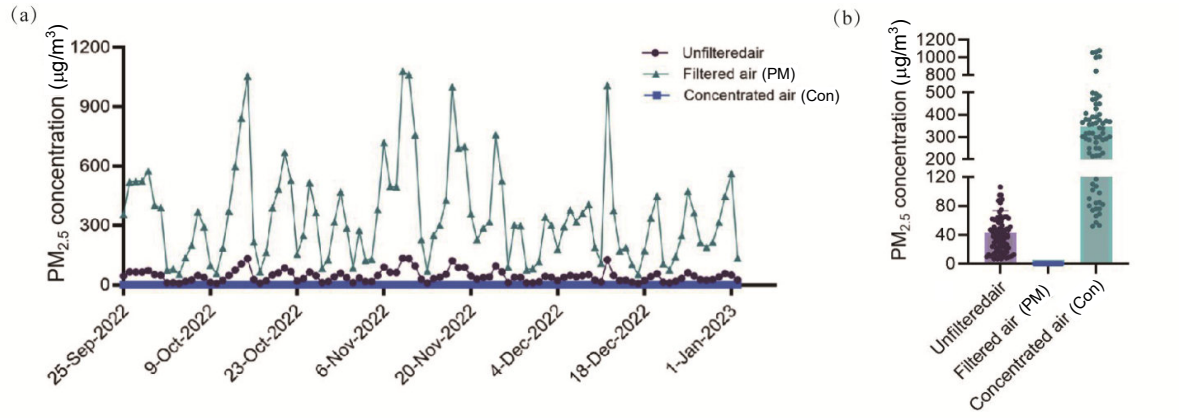

Fig. 1 The distribution of $PM_{2.5}$ concentrations within the exposure chambers during exposure duration.

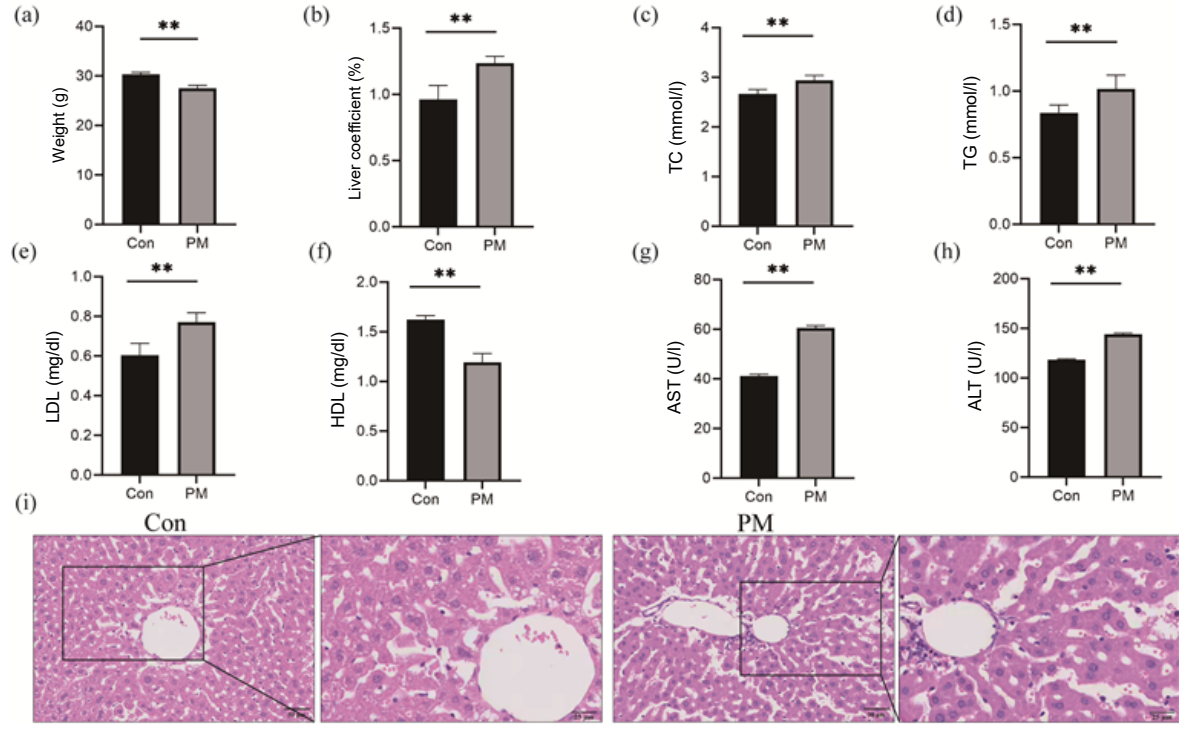

Fig. 2 Alterations in blood lipid biochemical parameters and HE staining in response to long-term exposure to $PM_{2.5}$. Parameters analyzed including (a) weight, (b) liver coefficient, (c) TC, (d) TG, (e) LDL, (f) HDL, (g) AST, and (h) ALT, $n = 6$. (i) HE staining performed for each group at a magnification of 200×. Pairwise comparisons were evaluated by the independent sample *t*-test. * $p < 0.05$ and ** $p < 0.01$.

by the detailed analysis of the results of WB and PCR as well as the brownish indication in IHC.

Caspase-1 inhibitors alleviate $PM_{2.5}$ induced hepatic disorder

As seen in Fig. 4 (a–h), a significant weight recovery and liver index decline were observed in the PV group compared with the PM group. The levels of AST, ALT, TC, TG, and LDL in serum decreased, and the level of HDL in serum increased significantly ($p<0.05$). The adverse effects of concentrated $PM_{2.5}$ air exposure on blood lipid profiles and liver function seem to be mitigated by treatment with caspase-1 inhibitors ($p<0.05$). The histological findings unequivocally demonstrate that hepatic injury and lipid accumulation in mouse livers exposed to $PM_{2.5}$ are effectively mitigated and reduced by the inhibition of caspase-1 such as using VX-765. In the PV group, cloudy swelling of hepatocytes

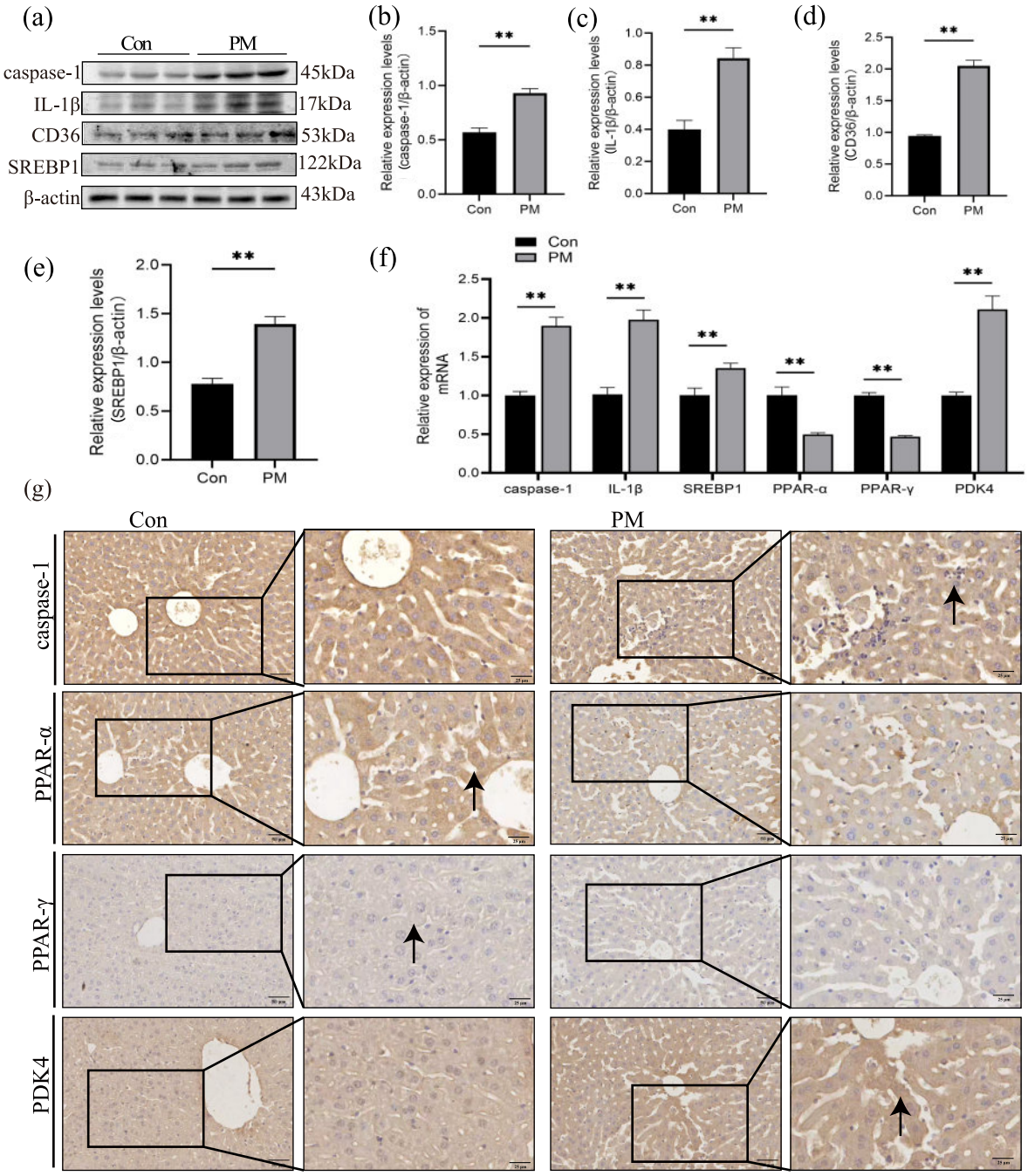

Fig. 3 Alterations in protein and transcriptional levels of factors related to lipid metabolism upon long-term exposure to $PM_{2.5}$. (a–e) Protein expression levels of caspase-1, IL-1β, CD36, and SREBP-1, $n = 3$. (f) mRNA expression levels of *caspase-1*, *CD36*, *SREBP-1*, *PPAR*-α, *PPAR*-γ, and *PDK4*, $n = 6$. (g) IHC revealing the expression of caspase-1, PPAR-α, PPAR-γ, and PDK4 in each group. Under a magnification of 200×, the black arrow indicates the positive area. The significant differences among multiple groups were evaluated by one-way ANOVA. * $p < 0.05$ and ** $p < 0.01$.

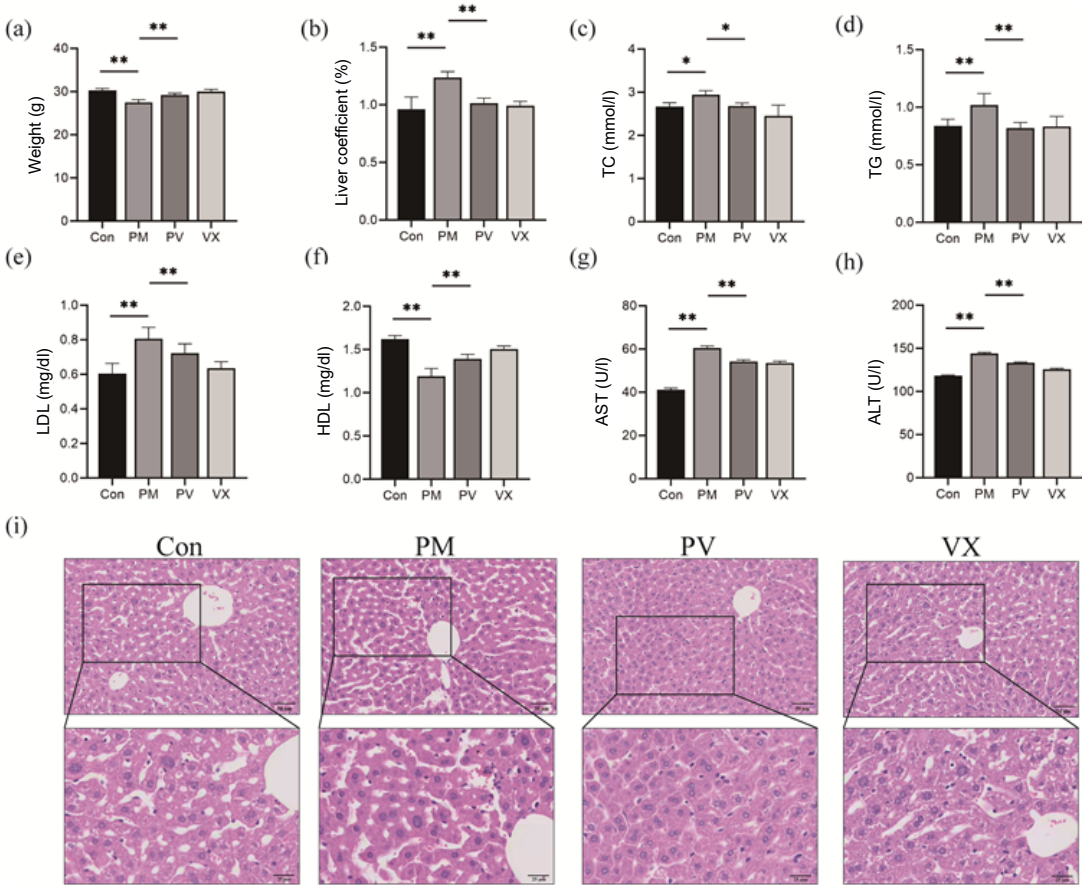

Fig. 4 Alterations in blood lipid biochemical parameters and HE staining in mice with long-term exposure to $PM_{2.5}$ after treatment with the caspase-1 inhibitor. Parameters analyzed including (a) weight, (b) liver coefficient, (c) TC, (d) TG, (e) LDL, (f) HDL, (g) AST, and (h) ALT, $n = 6$. (i) HE staining performed for each group at 200× magnification. The significant differences among multiple groups were evaluated by one-way ANOVA. * $p < 0.05$ and ** $p < 0.01$.

was significantly decreased with scattered inflammatory cell infiltration in hepatocytes, and a large number of lipid droplets decreased as shown in Fig. 4 (i). These results underscore the potential therapeutic efficacy of caspase-1 inhibition in mitigating $PM_{2.5}$-induced liver damage.

Caspase-1 inhibitors alleviate $PM_{2.5}$ activated lipid metabolic pathway promoting hepatic disorder

To further investigate the role of caspase-1 in $PM_{2.5}$ exposure-induced hepatic disorder, an intervention with VX-765 was conducted in the animal experiment. Additional theoretical support for the targeting of the caspase-1/IL-1β pathway has been provided by recent studies. In our study, the WB results demonstrated that, in comparison with the PM group, the protein expression levels of caspase-1, IL-1β, CD36, and SREBP-1 were decreased in the PV group ($p < 0.05$). The PCR results were in accordance with those of WB. Moreover, it was revealed that the transcript level of *PDK4* was decreased in the PV group relative to the PM group ($p < 0.05$), while the levels of *PPAR*-α and *PPAR*-γ were heightened ($p < 0.05$). As shown in Fig. 5, IHC results consistent with the trends of WB and PCR were observed. It is suggested that $PM_{2.5}$-induced metabolic dysregulation is alleviated by the administration of caspase-1 inhibitor. In summary, our study not only confirms the previous findings but also provides new evidence for the role of the caspase-1/IL-1β pathway in $PM_{2.5}$-induced hepatic disorder and lipid metabolism disorders, thereby further emphasizing the potential of caspase-1 inhibitors in regulating lipid metabolism and offering a therapeutic strategy to counteract the detrimental effects of $PM_{2.5}$ exposure on liver function and overall metabolic health.

DISCUSSION

Previous research has demonstrated that long-term exposure to $PM_{2.5}$ can induce hepatic steatosis and non-alcoholic fatty liver disease (NAFLD) in mice [12, 13].

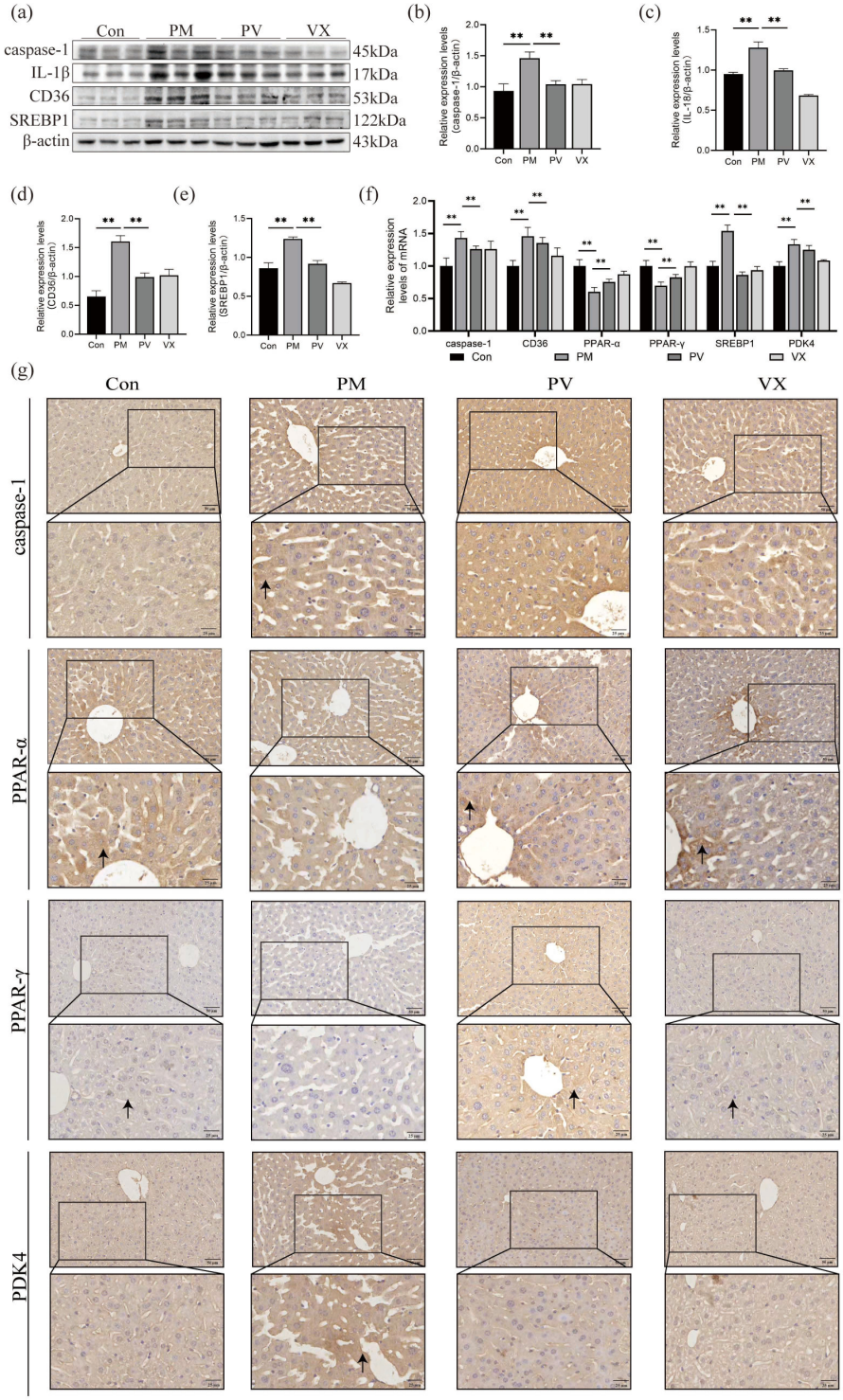

Fig. 5 Alterations in protein and transcriptional expression levels of lipid metabolism-related factors in mice with long-term $PM_{2.5}$ exposure upon treatment with the caspase-1 inhibitor. (a–e) Protein expression levels of caspase-1, IL-1β, CD36, and SREBP-1, $n = 3$. (f) mRNA expression levels of *caspase-1*, *CD36*, *SREBP-1*, *PPAR*-α, *PPAR*-γ, and *PDK4*, $n = 6$. (g) IHC revealing the expression of caspase-1, PPAR-α, PPAR-γ, and PDK4 in each group. Under a magnification of 200×, the black arrow indicates the positive area. The significant differences among multiple groups were evaluated by one-way ANOVA. * $p < 0.05$ and ** $p < 0.01$.

Given the pivotal role of the caspase-1 pathway in the adverse health effects associated with $PM_{2.5}$ and the variability of $PM_{2.5}$ physicochemical properties, this study focused on investigating the pro-inflammatory effects of $PM_{2.5}$ collected during the winter months and uncovering its underlying mechanisms. In our study, $PM_{2.5}$ was concentrated using an 8-fold concentration of the whole body dynamic exposure system of small animals in the Animal Experimental Center of the North China University of Science and Technology, and it was found that this concentrated $PM_{2.5}$ could influence liver lipid metabolism disorders through the caspase-1 pathway [14].

The caspase-1 inhibitor VX-765 was administered to mice by intraperitoneal injection at a dose of 50 mg/kg every 3 days for a total of 100 days. This extended treatment duration may introduce potential factors that could influence the research results. Multiple injections over such a long period could lead to injection stress, potentially affecting the physiological state of the mice [15]. This might result in alterations in behavior patterns or hormonal balance, subsequently influencing the metabolic processes of the liver and the overall response to the drug [16]. Additionally, local tissue damage caused by repeated injections may affect the absorption and distribution of the drug in the body, ultimately influencing the experimental results [17]. However, notwithstanding these potential concerns, our results suggest that the interference from these factors was not substantial enough to obscure the observed trends. This could be ascribed to the standardized injection procedure and the close surveillance of the mice, which contributed to ensuring that any potential interference was minimized [18]. Nevertheless, these potential interferences should be further explored by future studies to provide a more comprehensive understanding and to ensure the reliability and validity of the results.

To evaluate the impact of $PM_{2.5}$ exposure on the livers of mice, an online $PM_{2.5}$ concentration enrichment system was used to create an animal model. The exposed mice exhibited weight loss, increased liver index, and changes in biochemical markers, including elevated serum levels of TC, TG, AST, ALT, and LDL, and decreased HDL. Histopathology revealed destruction of the liver lobes, disordered arrangement of the liver plates, and fat vacuoles, suggesting hepatic disorder with lipid metabolic disorder following concentrated exposure to $PM_{2.5}$ [19].

To verify whether concentrated exposure to $PM_{2.5}$ air leads to lipid metabolic disorder, we measured the levels of caspase-1, IL-1β, CD36, SREBP-1, PPAR-α, PPAR-γ, and PDK4. These proteins are intricately involved in hepatic lipid disorders. SREBP-1 regulates lipogenesis by mediating the transcription of various lipogenic enzymes, thereby playing a crucial role in lipid metabolism [20]. PPAR-γ activation induces the transcription of many downstream lipogenic markers and primarily regulates a group of enzymes and proteins involved in fatty acid intake, transport, and oxidation, contributing to lipid homeostasis [21]. PDK4, a key lipid metabolism molecule, affects the expression of essential enzymes, thus influencing lipid metabolism pathways [22]. CD36, a multifunctional receptor that regulates fatty acid metabolism, promotes lipid binding and accumulation, affecting lipid distribution within the liver [23]. The cytokines IL-1β and caspase-1 dependent cytokines IL-16 and IL-18 seem to affect adipogenesis, adiposity, and lipid metabolism, highlighting their significance in lipid regulation. It is important to note that both IL-1β and caspase-1 are involved in the pyroptosis pathway, which has also been reported as a mechanism of $PM_{2.5}$ in cells [24]. This pyroptosis pathway may play an important role in the lipid metabolism disorder associated with $PM_{2.5}$ exposure. It could potentially interact with the functions of these proteins and further exacerbate the disruption of lipid metabolism. For example, the activation of the pyroptosis pathway might influence the activity of SREBP-1, PPAR-α, PPAR-γ, and other proteins involved in lipid metabolism, either directly or through the modulation of cytokine production [25]. However, the exact nature of these interactions and their implications for lipid metabolism require further investigation. In our study, a decrease in PPAR-α and PPAR-γ after $PM_{2.5}$ exposure was observed, which may be attributed to the following mechanisms. $PM_{2.5}$ may trigger oxidative stress and inflammation, which can interfere with the normal signaling pathways that regulate the expression of PPAR-α and PPAR-γ [26]. Additionally, the increased expression of cytokines and other factors in response to $PM_{2.5}$ exposure may downregulate these receptors [27]. This suggests that $PM_{2.5}$ is involved in and induces lipid metabolism disorder. However, the mechanism of lipid metabolism caused by caspase-1 still needs to be further deepened. Studies have reported that caspase-1 plays an important role in regulating lipid metabolism by coordinating the clearance of circulating triglycerides in healthy mice [28]. We intervened by intraperitoneal injection of the caspase-1 inhibitor VX-765 every 3 days and compared body weight, biochemical indicators, histopathological observations, and changes in lipid metabolism-related genes among the groups. The results showed that the caspase-1 inhibitor can improve hepatic disorder caused by $PM_{2.5}$. Moreover, changes in lipid metabolism-related genes indicated that caspase-1 can control inflammation-promoted hepatic disorder, fat transport and intake, and lipid binding and regulate key enzymes in lipid metabolism through pathways such as IL-1β, SREBP-1, PPARs, PDK4, CD36. When caspase-1 is activated, it may affect the secretion of IL-1β. Specifically, caspase-1 participates in the processing of the IL-1β precursor to make it an active form.

The active IL-1β then affects the differentiation of fat cells and the fat accumulation in the lipid metabolism process. This conclusion is in accordance with the findings of Vijayaraj et al and Akita et al [24, 29].

Caspase-1 may also affect the activity of SREBP-1. It may interact with the regulatory proteins related to SREBP-1 to change its conformation or its location in the cell, thereby affecting its activity. Caspase-1 may inhibit the degrading process of SREBP-1, increasing its concentration in the cell and mediating more transcription of fat-generating enzymes, ultimately affecting the synthesis of lipids. Those in agreement with our research findings include the reports from Niu et al and others [30, 31]. Caspase-1 may also inhibit the expression of PPAR-α and PPAR-γ. It may interact with the promoter region of the genes of PPAR-α and PPAR-γ or their transcriptional regulatory factors to interfere with the transcription process. Since PPAR-α and PPAR-γ play a crucial role in the oxidation of fatty acids, their inhibition affects the oxidation process of fatty acids and leads to an imbalance in lipid metabolism. The reduction in the expression of PPAR-α reduces the transcription of fatty acid oxidation-related enzymes, causing the accumulation of fatty acids in the cell and affecting the normal progress of lipid metabolism. In our research, the caspase-1 inhibitor is capable of elevating the protein expression levels of PPAR-α and PPAR-γ following long-term exposure to $PM_{2.5}$. This conclusion is in harmony with the findings of Grabacka et al and others [32–34]. In addition, caspase-1 may regulate the effect of CD36 in terms of fat transport and binding. It may phosphorylate or dephosphorylate CD36 to change its activity or its affinity for lipid molecules. When caspase-1 phosphorylates CD36, the binding ability of CD36 to fatty acids may be enhanced, promoting the binding of lipids to cells and affecting the transport and distribution of lipids in the body, ultimately changing the lipid metabolism process [35, 36]. Simultaneously, caspase-1 inhibitors can also inhibit lipid metabolism and transport to reduce lipid metabolic disorder. Therefore, targeted inhibition of caspase-1 might be a potential ideal drug for the treatment or prevention of $PM_{2.5}$-induced hepatic disorder.

However, this study still has certain limitations. Firstly, our research was conducted in the C57BL/6 mouse model. There is a possibility that long-term $PM_{2.5}$ exposure may trigger systemic inflammation in mice, leading to liver dysregulation. The observed effects of VX-765 treatment may be due to a reduction in systemic inflammation rather than being liver-specific. This model has certain limitations. Secondly, regarding the specific molecular mechanism by which caspase-1 inhibitors regulate lipid metabolism disorders, more in-depth exploration is still needed. This may involve the regulation of related signaling pathways such as the NF-κB and AMPK pathways, which will provide a theoretical basis for the development of more effective treatment strategies.

CONCLUSION

In conclusion, long-term exposure to $PM_{2.5}$ is associated with the occurrence of hepatic lipid metabolism disorders. In this study, a mouse model of a small animal whole-body dynamic exposure system was used to intervene, and it was shown that $PM_{2.5}$ exposure could induce liver lipid metabolism disorders in mice through caspase-1-mediated inflammatory response. Elucidating the mechanism of $PM_{2.5}$-induced hepatic lipid metabolism disorders provides useful information for the prevention and treatment of $PM_{2.5}$-associated liver diseases.

Appendix A. Supplementary data

Supplementary data associated with this article can be found at https://dx.doi.org/10.2306/scienceasia1513-1874.2025.028.

Acknowledgements: This study was funded by Hebei Provincial Department of Science and Technology Centrally Guided Local Development Fund Project (236Z7705G) and Natural Science Foundation of Hebei Province (C2022209003).

REFERENCES

1. Cohen AJ, Brauer M, Burnett R, Anderson HR, Frostad J, Estep K, Balakrishnan K, Brunekreef B, et al (2017) Estimates and 25-year trends of the global burden of disease attributable to ambient air pollution: an analysis of data from the Global Burden of Diseases Study (2015). *Lancet* **389**, 1907–1918.
2. Xiao Z, Li H, Gao Y (2022) Analysis of the impact of the Beijing-Tianjin-Hebei coordinated development on environmental pollution and its mechanism. *Environ Monit Assess* **194**, 91.
3. Yang Z, Mahendran R, Yu P, Xu R, Yu W, Godellawattage S, Li S, Guo Y (2022) Health effects of long-term exposure to ambient PM(2.5) in Asia-Pacific: A systematic review of cohort studies. *Curr Environ Health Rep* **9**, 130–151.
4. Mcduffie EE, Martin RV, Spadaro JV, Burnett R, Smith SJ, Rourke PO, Hammer MS, Donkelaar V, et al (2021) Source sector and fuel contributions to ambient PM(2.5) and attributable mortality across multiple spatial scales. *Nat Commun* **12**, 3594.
5. Zadoorian A, Du X, Yang H (2023) Lipid droplet biogenesis and functions in health and disease. *Nat Rev Endocrinol* **19**, 443–459.
6. Li R, Sun Q, Lam SM, Chen R, Zhu J, Gu W, Zhang L, Tian H, et al (2020) Sex-dependent effects of ambient PM(2.5) pollution on insulin sensitivity and hepatic lipid metabolism in mice. *Part Fibre Toxicol* **17**, 14.
7. Moonwiriyakit A, Dinsuwannakol S, Sontikun J, Timpratueang K, Muanprasat C, Khemawoot P (2024) Fine particulate matter $PM_{2.5}$ and its constituent, hexavalent chromium induce acute cytotoxicity in human airway epithelial cells via inflammasome-mediated pyroptosis. *Environ Toxicol Pharmacol* **107**, 104416.
8. Su P, Mao X, Ma J, Huang L, Yu L, Tang S, Zhuang M, Lu Z, et al (2023) ERRα promotes glycolytic metabolism

and targets the NLRP3/caspase-1/GSDMD pathway to regulate pyroptosis in endometrial cancer. *J Exp Clin Cancer Res* **42**, 274.
9. Wilson CH, Kumar S (2018) Caspases in metabolic disease and their therapeutic potentia. *Cell Death Differ* **25**, 1010–1024.
10. Wang L, Dong X, Feng S, Pan H, Jang X, Chen L, Zhao Y, Chen W, et al (2022) VX-765 alleviates dextran sulfate sodium-induced colitis in mice by suppressing caspase-1-mediated pyroptosis. *Int Immunopharmacology* **102**, 108405.
11. Xiao Q, Geng G, Xue T, Liu S, Cai C, He K, Zhang Q (2022) Tracking PM(2.5) and O(3) pollution and the related health burden in China 2013–2020. *Environ Sci Technol* **56**, 6922–6932.
12. Wu W (2023) Is air pollution joint prevention and control effective in China-evidence from "Air Pollution Prevention and Control Action Plan". *Environ Sci Pollut Res Int* **30**, 122405–122419.
13. Feng S, Gao D, Liao F, Zhou F, Wang X (2016) The health effects of ambient $PM_{2.5}$ and potential mechanisms. *Ecotoxicol Environ Saf* **128**, 67–74.
14. Zhao Y, Peng Y, Wang M, Zhao Y, He Y, Zhang L, Liu J, Zheng S (2024) Exposure to PM(2.5) and its constituents is associated with metabolic dysfunction-associated fatty liver disease: a cohort study in Northwest of China. *Environ Geochem Health* **46**, 304.
15. Leenaars M, Hendriksen CF (1998) Influence of route of injection on efficacy and side effects of immunisation. *Altex* **15**, 87.
16. Davis JN, Courtney CL, Superak H, Taylor DK (2014) Behavioral, clinical and pathological effects of multiple daily intraperitoneal injections on female mice. *Lab Anim (NY)* **43**, 131–139.
17. Hrycko A, Mateu GP, Ciervo C, Linn WR, Eckhardt B (2022) Severe bacterial infections in people who inject drugs: the role of injection-related tissue damage. *Harm Reduct J* **19**, 41.
18. Guarnieri M (2016) Considering the risks and safety of intraperitoneal injections. *Lab Anim (NY)* **45**, 131.
19. Xu MX, Ge CX, Qin YT, Gu TT, Lou DS, Li Q, Hu LF, Feng J, et al (2019) Prolonged $PM_{2.5}$ exposure elevates risk of oxidative stress-driven nonalcoholic fatty liver disease by triggering increase of dyslipidemia. *Free Radic Biol Med* **130**, 542–556.
20. Wu Y, Zheng W, Xu G, Zhu L, Li Z, Chen J, Wang L, Chen S (2024) C9orf72 controls hepatic lipid metabolism by regulating SREBP-1 transport. *Cell Death Differ* **31**, 1070–1084.
21. Cai W, YangT, Liu H, Han L, Zhang K, Hu X, Zhang X, Yin KJ, et al (2018) Peroxisome proliferator-activated receptor γ (PPARγ): A master gatekeeper in CNS injury and repair. *Prog Neurobiol* **163–164**, 27–58.
22. Cai W, Wang X, Deng Q, Gao J, Chen Y (2024) Expression and role of PDK4 on childhood dyslipidemia and lipid metabolism in hyperlipidemic mice. *Horm Metab Res* **56**, 167–176.
23. Chen Y, Zhang J, Cui W, Silverstein RL (2022) CD36, a signaling receptor and fatty acid transporter that regulates immune cell metabolism and fate. *J Exp Med* **219**, e20211314.
24. Vijayaraj SL, Feltham R, Rashidi M, Frank D, Liu Z, Simpson DS, Ebert G, Vince A (2021) The ubiquitylation of IL-1β limits its cleavage by caspase-1 and targets it for proteasomal degradation. *Nat Commun* **12**, 2713.
25. Yu P, Zhang X, Liu N, Tang L, Peng C, Chen X (2021) Pyroptosis: mechanisms and diseases. *Signal Transduct Target Ther* **6**, 128.
26. Montaigne D, Butruille L, Staels B (2021) PPAR control of metabolism and cardiovascular functions. *Nat Rev Cardiol* **18**, 809–823.
27. Vázquez CM, Wahli W (2022) PPARs as key mediators in the regulation of metabolism and inflammation. *Int J Mol Sci* **23**, 5025.
28. Molla MD, Akalu Y, Geto Z, Dagnew B, Ayelign B, Shibabaw T (2020) Role of caspase-1 in the pathogenesis of inflammatory-associated chronic noncommunicable diseases. *J Inflamm Res* **13**, 749–764.
29. Akita K, Ohtsuki T, Nukada Y, Tanimoto T, Namba M, Okura T, Takakura YR, Torigoe K, et al (1997) Involvement of caspase-1 and caspase-3 in the production and processing of mature human interleukin 18 in monocytic THP.1 cells. *J Biol Chem* **272**, 26595–26603.
30. Niu Z, Shi Q, Zhang W, Shu Y, Yang N, Chen B, Wang Q, Zhao X, et al (2017) Caspase-1 cleaves PPARγ for potentiating the pro-tumor action of TAMs. *Nat Commun* **8**, 766.
31. Wu S, Näär AM (2019) SREBP-1-dependent *de novo* fatty acid synthesis gene expression is elevated in malignant melanoma and represents a cellular survival trait. *Sci Rep* **9**, 10369.
32. Grabacka M, Pierzchalska M, Płonka PM, Pierzchalski P (2021) The role of PPAR alpha in the modulation of innate immunity. *Int J Mol Sci* **22**, 10545.
33. Mirza AZ, Althagafi II, Shamshad H (2019) Role of PPAR receptor in different diseases and their ligands: Physiological importance and clinical implications. *Eur J Med Chem* **166**, 502–513.
34. Nakagawa K, Tanaka N, Morita M, Sugioka A, Miyagawa S, Gonzalez FJ, Aoyama T (2012) PPARα is down-regulated following liver transplantation in mice. *J Hepatol* **56**, 586–594.
35. Li Y, Huang X, Yang G, Xu K, Yin Y, Brecchia G, Yin J (2022) CD36 favours fat sensing and transport to govern lipid metabolism. *Prog Lipid Res* **88**, 101193.
36. Zheng D, Liwinski T, Elinav E (2020) Inflammasome activation and regulation: toward a better understanding of complex mechanisms. *Cell Discovry* **6**, 36.

Appendix A. Supplementary data

Table S1 The details of reagents.

Reagent	Catalog	Brand	Location	Country
C57BL/6 SPF grade mice	SCXK (jing): 2020-0004	Huafukang Company	Beijing	China
Caspase-1 inhibitor VX-765	S2228	Selleck Chemicals	Houston	USA
Maintenance feed	1032	Huafukang Biotechnology Co., Ltd	Beijing	China
10×PBS	P102	Solarbio Science & Technology Co., Ltd	Beijing	China
Hematoxylin-eosin staining kit	C0105S	Solarbio Science & Technology Co., Ltd	Beijing	China
BCA quantification kits	P1200	Solarbio Science & Technology Co., Ltd	Beijing	China
SDS-PAGE Gel Kit	P1040	Solarbio Science & Technology Co., Ltd	Beijing	China
SDS-PAGE 5×loading buffer with DTT	T1081	Solarbio Science & Technology Co., Ltd	Beijing	China
Immobilon®-P PVDF Membrane	IPVH00005	Merck KGaA	Darmstadt	Germany
caspase-1 antibody	AF5418	Affinity Biosciences Ltd OH	Darmstadt	USA
IL-1β antibody	BF8021	Affinity Biosciences Ltd OH	Darmstadt	USA
PPAR-γ antibody	AF6284	Affinity Biosciences Ltd OH	Darmstadt	USA
CD36 antibody	PDF13262	Affinity Biosciences Ltd OH	Darmstadt	USA
SREBP-1 antibody	AF6283	Affinity Biosciences Ltd OH	Darmstadt	USA
PPAR-α antibody	66826-1-Ig	Proteintech group Inc	Wuhan	China
PDK4 antibody	12949-1-AP	Proteintech group Inc	Wuhan	China
β-actin antibody	66009-1-Ig	Proteintech group Inc	Wuhan	China
Rabbit IgG antibody	SA00001-2	Proteintech group Inc	Wuhan	China
Mouse IgG antibody	SA00001-1	Proteintech group Inc	Wuhan	China
ECL Enhanced Chemiluminescent Substrate	AP34L014	Lee Biosolutions Inc	Shanghai	China
Total RNA Extractor Kit	LS1040	Promega Corporation	Madison	USA
BlasTaq™ Probe 2×qPCR MasterMix	G890	Applied Biological Materials Inc	Vancouver	Canada
All-In-One 5×RT MasterMix	G592	Applied Biological Materials Inc	Vancouver	Canada
Two-step Universal Kit	PV-8000	ZSGB-Bio	Beijing	China

Table S2 The details of instruments.

Instrument	Catalog	Brand	Location	Country
Fully automatic biochemical analyzer	LABOSPECT008 AS	BioTek Instruments Inc	Tokyo	Japan
Dynamic inhalation exposure chambers of the exposure system	HRH-WBE10586	HuiRongHe Technology Inc	Beijing	China
Microplate spectrophotometer-Absorbance microplate detector for microplates	Epoch	BioTek Instruments Inc	Winooski	USA
Biological microscope	BM1000	Jiangnan Novel Optics Co., Ltd	Nanjing	China
WB developing instrument and chemiluminescence imaging system	ChemiScope 6100EXP	Chinon Scientific Instrument Co., Ltd	Shanghai	China
Electrophoresis tank	JY-ZY5	Junyi Oriental Electrophoresis Equipment Co Ltd	Beijing	China
Sanyo laboratory flake ice maker of of Panasonic	SIM-F140BDL	Panasonic Corporation Co., Ltd	Osaka	Japan
Electronic balance	Model AX223ZH/E	Ohaus Instruments Co. Ltd	Changzhou	China
Micro high-speed refrigerated centrifuge	Model 1730R	Gene Technology Co., Ltd	Wuhan	China
Universal electrophoresis power supply	Model JY300E	Junyi Oriental Electrophoresis Equipment Co., Ltd	Beijing	China
Gene amplification instrument	Model Biometra TOne 96G	Analytik Jena AG	Jena	Germany
PCR concentration detector and NanoDrop 2000/2000c Spectrophotometer system	Model V1.0 User Manual	Thermo Fisher Scientific	Massachusetts	USA
Real-time fluorescent quantitative gene amplification instrument	Model qTOWER^{3}G 230V	Thermo Fisher Scientific	Massachusetts	USA

Table S3 The sequences of relevant primers for RT-qPCR.

Gene	Forward Primer 5′–3′	Reverse Primer 5′–3′
caspase-1	CGAGGGTTGGAGCTCAAGTT	AGAAGTCTTGTGCTCTGGG
CD36	TGGGTTTTGCACATCAAAGA	GATGGACCTGCAAATGTCAGA
PPAR-α	TATTCGGCTGAAGCTGGTGTAC	CTGGCATTTGTTCCGGTTCT
PPAR-γ	TGGAAGCCTGATGCTTTATCCCCA	ATTCTGGCCCACCAACTTCGG
PDK4	TTCACACCTTCACCACATGC	ATCCCAGGTCGCTAGGACTTCAGG
β-actin	GATCTGGCACCACACCTTCT	GGGTGTTGAAGGTCTCAAA